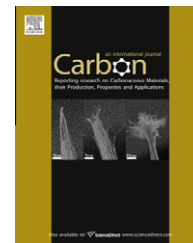


available at www.sciencedirect.comjournal homepage: www.elsevier.com/locate/carbon

Layer-by-layer synthesis of large-area graphene films by thermal cracker enhanced gas source molecular beam epitaxy

Ning Zhan, Mario Olmedo, Guoping Wang, Jianlin Liu *

Quantum Structures Laboratory, Department of Electrical Engineering, University of California, Riverside, CA 92521, United States

ARTICLE INFO

Article history:

Received 16 October 2010

Accepted 16 January 2011

Available online 23 January 2011

ABSTRACT

A thermal cracker enhanced gas source molecular beam epitaxy system was used to synthesize large-area graphene. Hydrocarbon gas molecules were broken by thermal cracker at very high temperature of 1200 °C and then impinged on a nickel substrate. High-quality, large-area graphene films were achieved at 800 °C, and this was confirmed by both Raman spectroscopy and transmission electron microscopy. A rapid cooling rate was not required for few-layer graphene growth in this method, and a high-percentage of single layer and bilayer graphene films was grown by controlling the growth time. The results suggest that in this method, carbon atoms migrate on the nickel surface and bond with each other to form graphene. Few-layer graphene is formed by subsequent growth of carbon layers on top of existing graphene layers. This is completely different from graphene formation through carbon dissolving in nickel and then precipitating from the nickel during rapid substrate cooling in the chemical vapor deposition method.

© 2011 Elsevier Ltd. All rights reserved.

1. Introduction

Graphene is a two dimensional carbon film with atoms densely packed together as hexagonal structure. Since it was discovered [1], graphene has attracted vast interests in condensed matter physics, chemistry, and nanotechnology communities due to its unique properties, such as extremely high mobility [2], anomalous quantum Hall effect [3,4], high mechanical strength, large thermal conductivity, good optical transparency, and high chemical stability [5]. Graphene may find many applications such as sensors, catalyst-support, composites, drug delivery, gas storage, energy storage and conversion, transparent conducting material, and post-silicon material for microelectronics industry.

Graphene has been synthesized by various methods. Solution/soft chemistry based synthesis methods such as solvothermal synthesis [6] and graphite oxide reduction [7] may lead to graphene materials with large volume and/or

small pieces, but not large and uniform thin sheets. These graphene films may be suitable for applications other than electronics. To use graphene for applications in nanoelectronics, it is essential to have large-area graphene substrates manufactured to tightly controlled specifications.

Currently, three major approaches are used to make large-area graphene. The first method is using mechanical exfoliation of graphite [1]. This method usually makes graphene with highest quality in terms of high electron mobility and low defect density, but the yield is very low and the approach is not suitable for commercialization. Second, graphitization of single crystal SiC was also used to produce ultrathin epitaxial graphite films by sublimation of Si from SiC substrate [4]. Graphene produced by this method is usually very fragile and contains many defects due to the large lattice mismatch between SiC substrate and graphene itself. Additionally, large-area production is also limited by the expensive SiC substrate. The third method is carbon precipitation from

* Corresponding author.

E-mail address: jianlin@ee.ucr.edu (J. Liu).

0008-6223/\$ - see front matter © 2011 Elsevier Ltd. All rights reserved.

doi:10.1016/j.carbon.2011.01.033

metal substrate [8–11]. Hydrocarbon gas is decomposed and dissolves into certain metals in a chemical vapor deposition (CVD) system. The dissolved carbon atoms segregate to metal surface and form thin graphitic layers as the substrate temperature cools [9]. Nickel [9–11] and copper [5,12] have been used as catalyst substrates in CVD system at high temperature (1000 °C). Due to this precipitation mechanism, very fast substrate cooling is needed; therefore, the accurate control of substrate temperature cooling rate is difficult. Additionally, the atmosphere or low-pressure process in CVD system may lead to over-saturation of carbon in metal substrate and subsequently make it difficult to control the number of layers of the as-grown films. Obviously, although having achieved a great deal of success, these methods still have various limitations and other methods to obtain uniform large-area graphene films are still desirable.

Here, thermal cracker enhanced gas source molecular beam epitaxy (GSMBE) graphene synthesis is proposed as an alternative method. The thermal cracker provides atomic carbon onto a metal surface, and these carbon atoms migrate on the surface to form graphene film directly. The direct growth of graphene on a surface is expected to possess better growth controllability than carbon precipitation for high quality and controllability of the number of layers.

2. Experimental

2.1. Sample growth and transfer

Three hundred nanometer SiO_2 covered n-type Si was used as substrate, and 300 nm nickel film was deposited by electron beam evaporation. After this deposition, the whole sam-

ple was transferred into a GSMBE system. Fig. 1a shows the diagram of this GSMBE chamber. The substrate is heated by a DC power supply. The thermal cracker is a spring-shaped tungsten filament with gas line coming through. Another DC power supply provides power to heat the filament. Typically, the tip and shell of the thermal cracker can reach 1200 and 550 °C, respectively. The bonds of gas molecules (acetylene) coming through the cracker are broken by high temperature, and carbon atoms are impinged onto the substrate for epitaxial growth. Acetylene was introduced after the target temperatures were reached. The flow speed was usually in the range of 5–10 sccm (standard cubic centimeters per minute). The sample was cooled at a rate of 10 °C/min after carbon growth for 6 min. Because graphene cannot be used as any field effect materials with conductive nickel underneath, a mild HCl solution (5%) was used to etch the nickel film. The sample was dipped into HCl solution for several hours. After the nickel film was etched away, graphene floated inside the solution and was ready to be transferred. The same SiO_2/Si substrate was put into the solution to lift the floating graphene slowly. To vaporize the water coming with the graphene, the sample was heated up to 100 °C for 10 min.

2.2. Characterization

High-resolution Philips CM300 TEM with electron gun voltage of 300 kV was used to characterize as-grown films. The Raman spectra were measured at room temperature with laser wavelength of 532 nm and power of 0.3 mW. The Veeco Dimension 5000 scanning probe microscope was used for atomic force microscope (AFM) measurement.

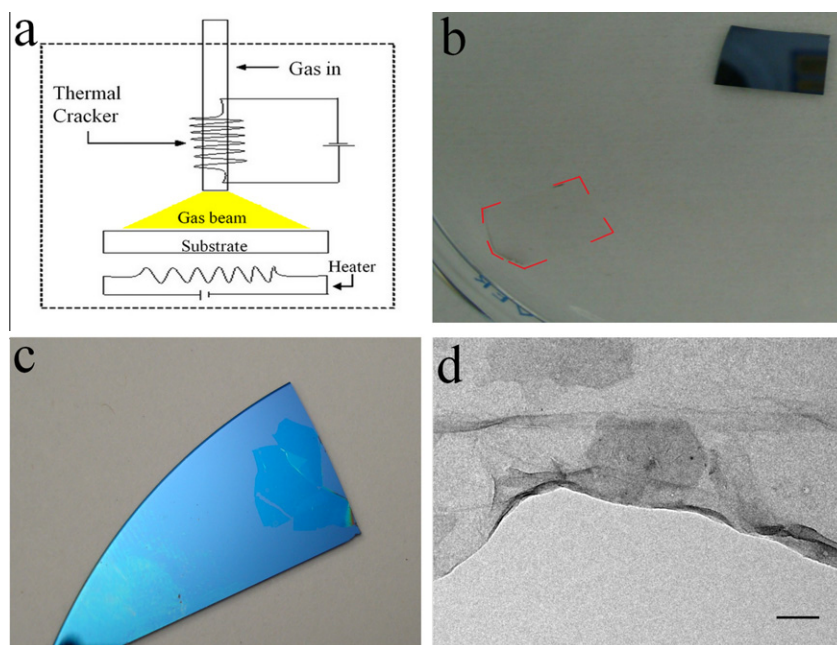


Fig. 1 – (a) Diagram of thermal cracker enhanced GSMBE system. (b) A floating graphene (shown in red polygon) after underneath nickel film was etched in 5% HCl solution. (c) A transferred graphene film on $\text{SiO}_2(300\text{ nm})/\text{Si}$ substrate. (d) Top-view TEM image of the graphene film (Scale bar is 100 nm). (For interpretation of the references in color in this figure legend, the reader is referred to the web version of this article.)

3. Results and discussion

Fig. 1b shows the graphene film grown at 800 °C floating in the 5% HCl solution after the nickel film was etched. Obviously, the graphene film can maintain its size and flatness after the metal film was etched. Fig. 1c shows an image of the transferred graphene film on SiO₂/Si substrate. The Van der Waals interaction guaranteed the graphene to strongly attach to the substrate. To understand the surface morphology of graphene, a top-view transmission electron microscopy (TEM) image was taken and shown in Fig. 1d. It shows clear contrast between areas with different thicknesses of graphene. This variation of number of layers is mainly due to the formation of nickel grains. A similar phenomenon was also found for CVD growth [9–11].

After transferring graphene to the SiO₂/Si substrate, micro-Raman analysis was used to characterize the graphene film with the laser wavelength of 532 nm. G band (~1580 cm⁻¹) and 2D band (2700 cm⁻¹), which are the most prominent phonon features of graphene film, were found (Fig. 2a). Negligible D band (~1350 cm⁻¹) indicates the high quality of graphene films with very few defects. The thin sections of graphene, which correspond to the bright parts in Fig. 1d, have two major types of curves shown as the bottom two curves in Fig. 2a. The ratio between G band and 2D band (I_G/I_{2D}) can be used to distinguish the number of layers for as-grown graphene samples [11]. The small ratios of 0.28 and 1 for these two curves correspond to single layer and bilayer graphene films, respectively, which occupy almost 70% of the whole film. The Raman spectroscopy of dark parts of the film is also shown as the third curve from the bottom in Fig. 2a. The bigger I_G/I_{2D} ratio of 1.57 indicates three-layer graphene for these dark parts. For some parts of film especially on boundaries between nickel grains, a I_G/I_{2D} ratio of more than 1.8 was found (the top curve in Fig. 2a). Because of the limitation of the Raman scattering method [11], a ratio bigger than 1.8 cannot be used to tell how many layers exactly the film has. Fig. 2b shows an AFM image of the transferred film. The variation of the contrast in the image indicates different thickness of layers. The height measurement profile (Fig. 2c) of the cross section indicated by the arrow in Fig. 2b shows that the thickness of the film is around 0.8 nm, suggesting single-layer graphene in this selected area [11]. Different grains cause different number of layers during growth, and the boundaries between grains have thermal stress induced by the terraces-like steps [9]. Hence, the graphene films on boundaries tend to grow vertically and form as wrinkles, which can be seen as bright lines in the AFM image (Fig. 2b).

In conjunction with Raman scattering and AFM characterization, TEM measurement was carried out. The graphene was transferred to TEM copper grid by the same method as if it was transferred onto the SiO₂/Si substrate. A lacy copper grid without any carbon film was chosen and dipped into HCl solution. After the floating graphene was lifted up, remaining water on the grid was naturally vaporized. The graphene tends to fold back, which gives a convenient way to take a cross-section view. Single-layer, bilayer, trilayer and multi-layer graphene were all found by TEM (Fig. 3a–d). The inter-layer distance of about 3.4 Å was estimated by fast Fourier transform, which agrees with the interlayer distance of

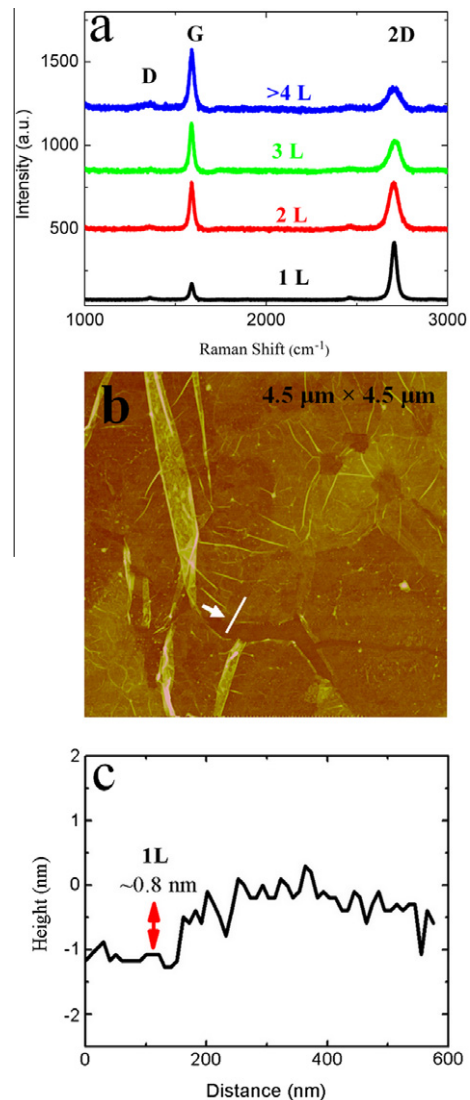


Fig. 2 – (a) Raman spectra of graphene films grown at 800 °C by thermal cracker enhanced GSMBE. Curves correspond to single layer, bilayer, triple layer and multi-layer graphene from the bottom to the top. (b) AFM image of the sample. (c) Height measurement profile of the cross section indicated by the arrow in (b).

graphite. Furthermore, the diffraction pattern of most parts of films has a very clear hexagonal pattern, which confirms the three-fold symmetry of the arrangement of carbon atoms (Fig. 3e). This also agrees with the high quality of the film derived by the Raman spectra. Besides this major hexagonal diffraction enhanced spots, some part of the film also has secondary hexagonal enhanced spots shown in Fig. 3f. Two reasons might contribute to this phenomenon. On one hand, because the graphene films tend to fold back randomly, there is great chance that some films stack together as the one shown in Fig. 3g, which has four individual films folded together. On the other hand, the secondary sets of spots can originate from the mis-stacked order of individual films. Graphene films exfoliated from HOPG are stacked in AB Bernal stacking order (Fig. 3h), where the vacant centers of the

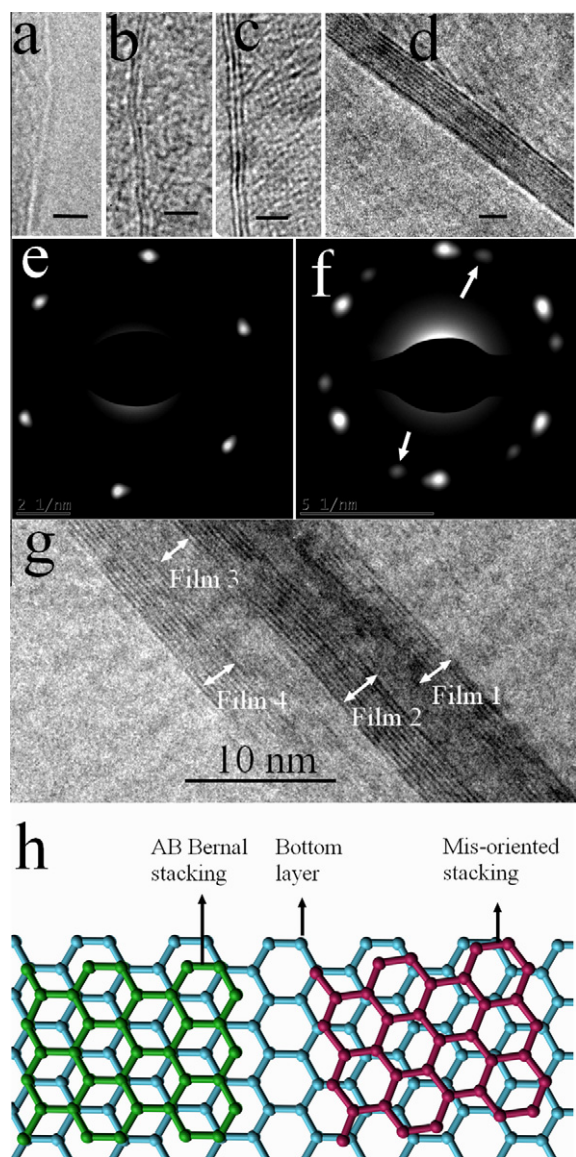


Fig. 3 – Cross-sectional TEM images of (a) Single-layer, (b) Bi-layer, (c) Tri-layer and (d) Multi-layer graphene. The scale bar is 2 nm. (e) Diffraction pattern of as-grown sample. (f) Diffraction pattern of certain part of the film has the second sets of spots as shown by arrows. (g) Several films stacking together. (h) Illustration of AB Bernal stacking graphene (green) and mis-oriented stacking graphene (red). (For interpretation of the references in color in this figure legend, the reader is referred to the web version of this article.)

hexagons on one layer have carbon atoms on hexagonal corner sites on the two adjacent graphene layers along c-axis. Depending on growth conditions, different layers in as-grown graphene films may not be stacked together according to AB Bernal stacking order; they could be stacked in a mis-oriented stacking order (Fig. 3h). This can be proved from Raman scattering results (Fig. 2a). If the graphene films adopt AB Bernal stacking order, the profile of 2D band should evolve with different number of layers, and it was noticed that only 2D band of single layer graphene films has Lorentzian feature [13]. But for the Raman spectra obtained here, even the films of more

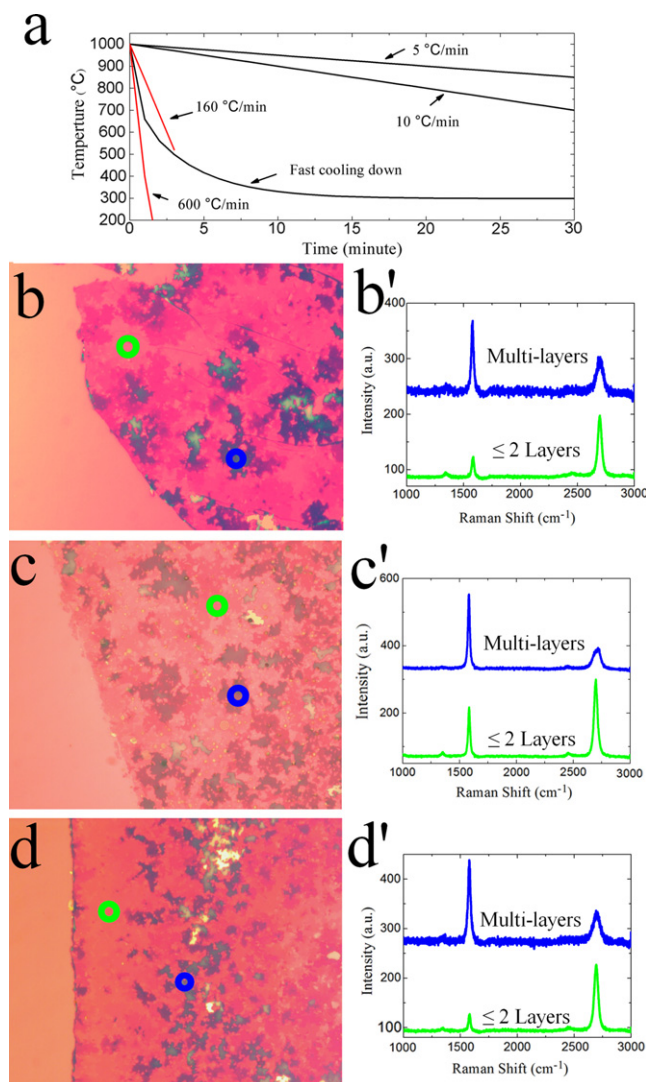


Fig. 4 – (a) Different cooling rates. 160 and 600 °C/min (shown in red lines) cooling were used by CVD method [9,10,15,16]. Fast cooling, 10 and 5 °C/min cooling were tested in the thermal cracker enhanced GSMBE for comparison. Optical microscopy images (b, c and d) and corresponding Raman spectra (b', c' and d') of as-grown graphene films with different cooling rates on 300 nm SiO₂/Si substrates. (b) Fast cooling as shown in (a). (c) 10 °C/min cooling. (d) 5 °C/min cooling. Representative positions where Raman spectra are taken are identified by circles in corresponding color in optical images. (For interpretation of the references in color in this figure legend, the reader is referred to the web version of this article.)

than one layer have Lorentzian distributed 2D band, while the full width at half maximum (FWHM) increases with the number of layers. FWHM varies as 34, 62, 69 and 94 cm⁻¹ for single-layer, bi-layer, tri-layer and multilayer graphene, respectively (Fig. 2a). This is due to the weak interaction between adjacent mis-oriented layers [14]. Therefore, both the Raman spectra and diffraction patterns may be used to predict the stacking order of as-grown graphene films.

Although still controversial, the over-saturated carbon atoms precipitate to metal surface to form graphene at lower

temperature in CVD process. Rapid substrate cooling rate is found in many CVD processes to suppress the formation of multi-layers or even graphite and obtain few layers graphene. Typically, 160 °C/min [9] and 600 °C/min [10,15,16] were tried and proved to be necessary for growth of a few layers. To verify the growth mechanism of our thermal cracker enhanced GSMBE system, different cooling rates were investigated. Fig. 4a shows the comparison of cooling rates used in CVD method (shown in red lines) from the literature and our GSMBE system. Fast cooling in between 160 and 600 °C/min, 10, and 5 °C/min were chosen as different cooling rates at a growth temperature of 1000 °C in our experiments. Figs. 4b–d shows the optical microscopy images of graphene films, which were grown with these different cooling rates and subsequently transferred onto 300 nm SiO₂/Si substrates. Because the optical contrast is interfered by the thickness of graphene film, different parts of a graphene sample with the same optical contrast should have the same number of layers. To identify the number of layers in the light red parts of these samples, micro-Raman spectra were carried out on certain positions enclosed by green circles in the optical images. The corresponding Raman curves are shown in green in the right side of each image, which all have a I_G/I_{2D} ratio less than one, indicating single-layer or bilayer graphene film. Other dark parts (enclosed by blue circles) of these samples have much bigger I_G/I_{2D} ratio (shown in blue color in the right side of each image), suggesting the formation of multi-layer graphene. From the optical images of these samples, the percentage of single-layer and bilayer graphene are approximately 75%, 70% and 74% for fast cooling, 10 and 5 °C/min, respectively. Fast cooling and very slow cooling do not have obvious difference for graphene growth in the thermal cracker enhanced GSMBE system, therefore rapid cooling is not required for thermal cracker enhanced MBE growth.

To further investigate the mechanism of thermal cracker enhanced GSMBE growth, different growth times were tested. Fig. 5 shows optical microscopy images of transferred samples on SiO₂/Si substrate with the growth time of 1, 4, 6 and 10 min, respectively. All other growth conditions were kept the same, including the substrate temperature of 800 °C, cooling rate of 10 °C/min, etc. For the sample with only 1 min growth, the as-grown carbon layer is not a film yet but a porous net (Fig. 5a). With the increase of growth time, more and more carbon atoms grow into porous net and form a continuous film (Figs. 5b and c). As the growth time reaches 10 min (Fig. 5d), the film becomes a very dense carbon film with much higher contrast compared to SiO₂, which means most parts of film already had become multi-layers graphene or even graphite. Therefore, it is not the different cooling rates but the growth time that manipulate the number of layers of the grown films in the GSMBE system. This means we observe traditional growth of one layer on top of another carbon layer, rather than graphene growth of one layer at the bottom of another carbon layer in CVD method.

To verify the direct growth mechanism from a different angle, graphene films were also grown at different temperatures of less than 800 °C in our GSMBE system, which are normally too low to form any graphene in CVD method. Fig. 6a–d show the evolution of Raman spectra for graphene films grown at temperatures from 750 to 600 °C. As the temperature decreases from 800 to 750 °C, an obvious defect peak appears. The ratio between D peak and G peak is usually used to indicate the amount of defects. The value for 750 °C sample is 0.58 which demonstrates a large amount of defects in the films, and it increases to 0.8 for the sample grown at 700 °C. As the substrate temperature keeps decreasing, the D peak still exists and gradually merges into G peak. Additionally, the 2D peak, which is supposed to be around 2700 cm⁻¹, does not ap-

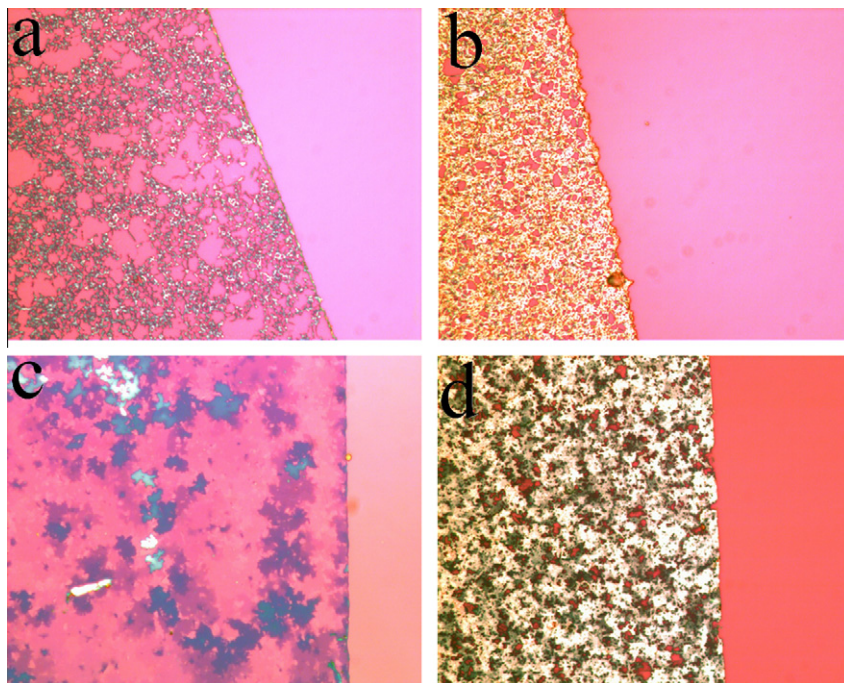


Fig. 5 – Optical microscopy images of as-grown graphene films with different growth time on the 300 nm SiO₂/Si substrate. (a) 1 min, (b) 4 min, (c) 6 min, (d) 10 min.

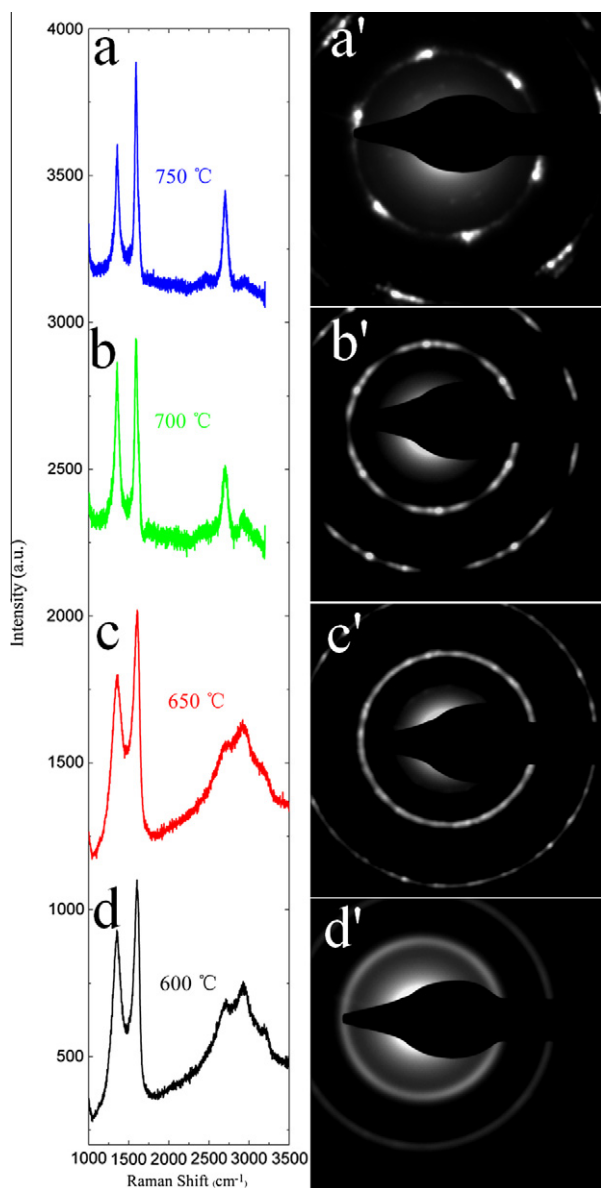


Fig. 6 – Evolution of Raman spectra (a, b, c and d) and corresponding diffraction patterns (a', b', c' and d') for graphene films grown at different temperatures. (a) 750 °C, (b) 700 °C, (c) 650 °C and (d) 600 °C.

pear anymore; instead, a big “wave packet” occurs from 2500 to 3200 cm^{-1} for 650 and 600 °C samples. This is a typical indication of carbon amorphization [17]. Corresponding TEM diffraction patterns of these films are shown in Fig. 6a'–d'. The diffraction pattern for 800 °C sample (Fig. 3e) has a very clear hexagonal pattern agreeing with the high quality of the film derived by the Raman spectrum. The diffraction pattern starts to appear as ring-like shape besides hexagonal pattern for 750 °C sample (Fig. 6a'), it should be due to the fact that the film starts to become more polycrystalline and adjacent layers start to distribute more randomly, which brings more defects also indicated in Raman spectrum. From 650 and 600 °C samples, the hexagonal pattern disappears and the ring-like shape occurs (Fig. 6c' and d'). This proves that the films are already starting to be amorphous at these temperatures, which

agrees with Raman spectra of these samples. Two major reasons may contribute to this evolution. On one hand, the decrease of temperature causes insufficient thermal energy provided by substrate and decrease the diffusion length of carbon atoms on the nickel surface. Instead of forming as “graphitic” carbon, the carbon atoms reconstruct as other forms, such as relaxed dislocation geometries for vacancy units [18] or “carbodic” carbon [19,20], which have less formation energy. Further decrease of substrate temperature to 650 °C and below results in the fact that these carbon atoms cannot have enough energy to form any crystals. On the other hand, the lower the temperature is, the rougher the nickel surface is. Because nickel film provides the supporting template for carbon to form graphene, rougher surface obviously prevents the carbon atoms from diffusing freely, leading to compromised quality.

In the CVD method, the graphene is formed in the cooling period; by contrast, the results above indicate that the thermal cracker enhanced GSMBE system forms graphene during the hydrocarbon gas inputting period. The high-temperature thermal cracker breaks the gas molecules into atoms, the carbon atoms are impinged on the nickel surface. While portion of these atoms may be dissolved into the nickel film, many carbon atoms are adsorbed on the nickel surface and diffuse around. A complete graphene layer can be formed by these adsorbed carbon atoms fitting the hollow sites of the substrate [19,20]. Once the nickel surface is covered by this graphitic carbon layer, the catalytic activity of nickel film is greatly reduced [19]. This as-grown graphene layer provides the template for further layer by layer growth. Therefore, nickel films mainly serve as adsorption sites for the graphene growth in this method rather than as catalyst in CVD method. This leads to a key difference between CVD method and thermal cracker enhanced GSMBE method in terms of when graphene films are formed. The thermal cracker enhanced GSMBE method has tremendous potential for controllable growth of graphene with different layers. Depending on the substrate temperature and the flatness of the substrate, the graphene film may be quickly formed. The as-grown graphene suppresses further dissolving carbon into nickel film, which would never become carbon saturation. Therefore, during the substrate cooling, no carbon atoms may segregate onto the nickel surface to form additional graphene layers. This suggests that different cooling rates have no effect on the formation of graphene, as shown earlier.

4. Conclusions

Large-area, few-layer graphene films were synthesized by thermal cracker enhanced GSMBE, and the growth mechanism was found to differ from that of CVD. The quality of as-grown graphene films was controlled by the growth time rather than the cooling rate. Large-area, few-layer graphene films were achieved at 800 °C, about 200 °C lower than the temperature used in the typical CVD method. Clear diffraction patterns indicate a high-quality hexagonal structure. The profile of the 2D bands and diffraction patterns prove the mis-oriented stacking order of as-grown films. More defects in the graphene film occur at lower growth temperature;

it becomes amorphous carbon when the temperature reaches 650 °C. These results suggest that graphene has been synthesized on the nickel substrate through layer-by-layer growth mode.

Acknowledgments

The authors would like to thank the center of nanomaterials and nanodevices funded by the Defense Microelectronics Activity (DMEA) under the agreement number H94003-10-2-1003.

REFERENCES

- [1] Novoselov KS, Geim AK, Morozov SV, Jiang D, Zhang Y, Dubonos SV, et al. Electric field effect in atomically thin carbon films. *Science* 2004;306(5696):666–9.
- [2] Bolotin KI, Sikes KJ, Jiang Z, Klima M, Fudenberg G, Hone J, et al. Ultrahigh electron mobility in suspended graphene. *Solid State Commun* 2008;146(9):351–5.
- [3] Novoselov KS, Geim AK, Morozov SV, Jiang D, Katsnelson MI, Grigorieva IV, et al. Two-dimensional gas of massless Dirac fermions in graphene. *Nature* 2005;438(7056):197–200.
- [4] Berger C, Song Z, Li X, Wu X, Brown N, Naud C, et al. Electronic confinement and coherence in patterned epitaxial graphene. *Science* 2006;312(5777):1191–6.
- [5] Li X, Zhu Y, Cai W, Borysiak M, Han B, Chen D, et al. Transfer of large-area graphene films for high-performance transparent conductive electrodes. *Nano Lett* 2009;9(12):4359–63.
- [6] Choucair M, Thordarson P, Stride JA. Gram-scale production of graphene based on solvothermal synthesis and sonication. *Nature Nanotech* 2009;4:30–3.
- [7] Stankovich S, Dikin DA, Dommett GHB, Kohlhaas KM, Zimney EJ, Stach EA, et al. Graphene-based composite materials. *Nature* 2006;442(7100):282–6.
- [8] Land TA, Michely T, Behm RJ, Hemminger JC, Comsa G. STM investigation of single layer graphite structures produced on Pt(111) by hydrocarbon decomposition. *Surf Sci* 1992;264(3):261–70.
- [9] Chae SJ, Güne F, Kim KK, Kim ES, Han GH, Kim SM, et al. Synthesis of large-area graphene layers on poly-nickel substrate by CVD wrinkle formation. *Adv Mater* 2009;21(22):2328–33.
- [10] Kim KS, Zhao Y, Jang H, Lee SY, Kim JM, Kim KS, et al. Large-scale pattern growth of graphene films for stretchable transparent electrodes. *Nature* 2009;457(7230):706–10.
- [11] Reina A, Jia X, Ho J, Nezich D, Son H, Bulovic V, et al. Large area, few-layer graphene films on arbitrary substrates by chemical vapor deposition. *Nano Lett* 2009;9(1):30–5.
- [12] Li X, Cai W, An J, Kim S, Nah J, Yang D, et al. Large-area synthesis of high-quality and uniform graphene films on copper foils. *Science* 2009;324(5932):1312–4.
- [13] Ferrari AC, Meyer JC, Scardaci V, Casiraghi C, Lazzeri M, Mauri F, et al. Raman spectrum of graphene and graphene layers. *Phys Rev Lett* 2006;97(18):187401–3.
- [14] Malard LM, Pimenta MA, Dresselhaus G, Dresselhaus MS. Raman spectroscopy in graphene. *Phys Rep* 2009;473(5):51–87.
- [15] Lee Y, Bae S, Jang H, Jang S, Zhu S, Sim SH, et al. Wafer-scale synthesis and transfer of graphene films. *Nano Lett* 2009;10(2):490–3.
- [16] Son DI, Kim TW, Shim JH, Jung JH, Lee DU, Lee JM, et al. Flexible organic bistable devices based on graphene embedded in an insulating poly(methyl methacrylate) polymer layer. *Nano Lett* 2010;10(7):2441–7.
- [17] Dresselhaus MS, Jorio A, Hofmann M, Dresselhaus G, Saito R. Perspectives on carbon nanotubes and graphene Raman spectroscopy. *Nano Lett* 2010;10(3):751–8.
- [18] Jeong BW, Ihm J, Lee G. Stability of dislocation defect with two pentagon-heptagon pairs in graphene. *Phys Rev B* 2008;78(16):165403.
- [19] Papagno L, Caputi LS. Determination of graphitic carbon structure adsorbed on Ni(1 1 0) by surface extended energy-loss fine-structure analysis. *Phys Rev B* 1984;29(3):1483–6.
- [20] Rosei R, Crescenzi MD. Structure of graphitic carbon on Ni(1 1 1): a surface extended-energy-loss fine-structure study. *Phys Rev B* 1983;28(2):1161–4.